Scholars Research Library

Der Pharmacia Lettre, 2016, 8 (4):212-224
(http://scholarsresearchlibrary.com/archive.html)

ISSN 0975-5071
USA CODEN: DPLEB4

Anti-corrosive properties of Sulfamethoxypyridazine on mild steel corrosion in 2M H_3PO_4 solution: Experimental and theoretical studies

L. Adardour[1,2], H. Lgaz[1, 3], R. Salghi[3*], M. Larouj[1], S. Jodeh[4,*], M. Zougagh[5,6], O. Hamed[4] and H. Oudda[1]

[1]Laboratory separation processes, Faculty of Science, University IbnTofail PO Box 242, Kenitra, Morocco
[2]Laboratoire d'Ingénierie de Modélisation et d'Environnement, Faculté des Sciences Dhar El Mehraz FES B.P. 1796 Atlas Fès Maroc
[3]Laboratory of Applied Chemistry and Environment, ENSA, Université Ibn Zohr, PO Box 1136, 80000 Agadir, Morocco
[4]Department of Chemistry, An-Najah National University, P. O. Box 7, Nablus, Palestine
[5]Regional Institute for Applied Chemistry Research, IRICA, E-13004, Ciudad Real, Spain
[6]Castilla-La Mancha Science and Technology Park, E-02006, Albacete, Spain

---

ABSTRACT

The inhibition effect of Sulfamethoxypyridazine(SMP) against mild steel corrosion in 2.0 M H3PO4 was evaluated using weight loss and electrochemical techniques (potentiodynamic polarization and electrochemical impedance). The experimental results showed that SMP is a good corrosion inhibitor and the inhibition efficiency increased with the increase of SMP concentration, while the adsorption followed the Langmuir isotherm. Theoretical calculation was carried out to establish mechanism of corrosion inhibition for mild steel with SMP in 2.0 M H3PO4 medium. The inhibition action of the compound was assumed to occur via adsorption on the steel surface through the active centers in the molecule. The corrosion inhibition is due to the formation of a chemisorbed film on the steel surface.

Keywords: Corrosion inhibitor; Sulfamethoxypyridazine; Mild steel; DFT; Phosphoric acid; EIS

INTRODUCTION

Mild steel as one kind of engineering structural materials, is employed in tonnages in offshore engineering, chemical processing, petroleum production and refining pipelines, mining and construction, etc. It has good mechanical, physical, and chemical properties, such as plastic, toughness, welding, stamping and cutting performance, etc[1]–[7]. Phosphoric acid prepared by dihydrate and hemihydrate wet processes generate severe corrosion problems in containers. In order to prevent corrosion, the primary strategy adopted is to isolate the metal from corrosive medium. Amongst the various methods available, the use of inhibitors is one of the most practical methods for protection against corrosion[8]–[10].

The use of organic compounds containing oxygen, sulphur and nitrogen to reduce corrosion attack on steel has been studied in some details. These compounds get adsorbed onto the surface of metal from the bulk of environment forming a film at the metal surface. The efficiency of organic inhibitors depends on their structure, especially chemical/electronic structure[8]–[12]. Those structural parameters can be obtained from quantum chemical methods, which have been extensively used to study reaction mechanism. Several groups[13]–[17] have studied the inhibition mechanism of some organic molecules by quantum chemical calculations, has successfully been established to probe the relationship between the quantum chemical parameters of inhibitor molecule and inhibition efficiency.

In this paper, the corrosion inhibition performance of Sulfamethoxypyridazine(SMP) for mild steel in phosphoric acid solutions was investigated by weight loss and electrochemical techniques. Density Functional Theory (DFT) calculations were performed to study the electronic structure and the adsorption of SMP onto mild steel. Figure 1 shows the molecular structure of the SMP utilized in this investigation:

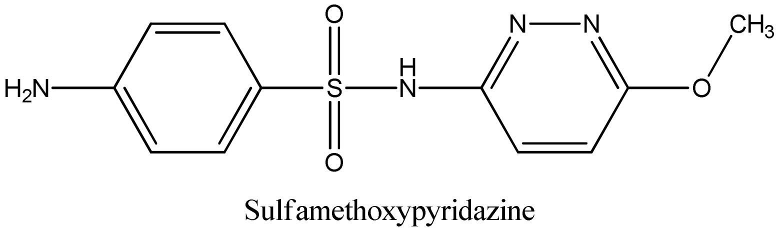

Figure 1. Molecular structure of studied compound

MATERIALS AND METHODS

Materials

The steel used in this study is a carbon steel (Euronorm: C35E carbon steel and US specification: SAE 1035) with a chemical composition (in wt%) of 0.370 % C, 0.230 % Si, 0.680 % Mn, 0.016 % S, 0.077 % Cr, 0.011 % Ti, 0.059 % Ni, 0.009 % Co, 0.160 % Cu and the remainder iron (Fe). The carbon steel samples were pre-treated prior to the experiments by grinding with emery paper SiC (120, 600 and 1200); rinsed with distilled water, degreased in acetone in an ultrasonic bath immersion for 5 min, washed again with bidistilled water and then dried at room temperature before use.

Solutions

The aggressive solutions of 2.0 M H_3PO_4 was prepared by dilution of analytical grade 37% HCl with distilled water. The concentration range of Sulfamethoxypyridazine used was 5×10^{-4}M to 1×10^{-5}M.

Corrosion tests

The gravimetric measurements were carried out at definite time interval of 6 h using an analytical balance (precision ± 0.1 mg), The surface of the test electrode was mechanically abraded by different grades of emery papers with 220 up to 1500, washed with distilled water, cleaned with acetone after being weighed accurately with high sensitivity balance, the specimens were carried out in a double glass cell equipped with a thermostated cooling condenser containing 80 mL of non-de-aerated test solution with and without various concentrations of the studied SMP at 303K. After immersion period, the specimens were taken out, rinsed thoroughly with bidistilled water, dried and weighed accurately again. Five tests were performed in each case and the mean value of the weight loss was calculated.

The electrochemical measurements were carried out using Volta lab (Tacussel- Radiometer PGZ 100) potentiostate and controlled by Tacussel corrosion analysis software model (Volta master 4) at under static condition. The corrosion cell used had three electrodes. The reference electrode was a saturated calomel electrode (SCE). A platinum electrode was used as auxiliary electrode of surface area of 1 cm^2. The working electrode was carbon steel. All potentials given in this study were referred to this reference electrode. The working electrode was immersed in test solution for 30 minutes to a establish steady state open circuit potential (E_{ocp}). After measuring the E_{ocp}, the electrochemical measurements were performed. All electrochemical tests have been performed in aerated solutions at 298 K. The EIS experiments were conducted in the frequency range with high limit of 100 kHz and different low limit 100 mHz at open circuit potential, with 10 points per decade, at the rest potential, after 30 min of acid immersion, by applying 10 mV ac voltage peak-to-peak. Nyquist plots were made from these experiments. The best semicircle can be fit through the data points in the Nyquist plot using a non-linear least square fit so as to give the intersections with the x-axis.

The electrochemical behaviour of carbon steel sample in inhibited and uninhibited solution was studied by recording anodic and cathodic potentiodynamic polarization curves. Measurements were performed in the 2.0 M H_3PO_4 solution containing different concentrations of the tested inhibitor by changing the electrode potential automatically from - 800 to -200 mV versus corrosion potential at a scan rate of 2 $mV.s^{-1}$. The linear Tafel segments of anodic and cathodic curves were extrapolated to corrosion potential to obtain corrosion current densities (I_{corr}).

Computational procedures

Complete geometrical optimizations of the investigated molecules are performed using DFT (density functional theory) with the Beck's three parameter exchange functional along with the Lee-Yang-Parr nonlocal correlation functional (B3LYP)[18]–[20] with 6-31G(d) basis set is implemented in Gaussian 03 program package[21]. This approach is shown to yield favorable geometries for a wide variety of systems. This basis set gives good geometry optimizations. The geometry structure was optimized under no constraint. The following quantum chemical parameters were calculated from the obtained optimized structure: The highest occupied molecular orbital (E_{HOMO}) and the lowest unoccupied molecular orbital (E_{LUMO}), the energy difference (ΔE) between E_{HOMO} and E_{LUMO}, dipole moment (µ), electron affinity (E*A*), ionization potential (*I*) and the fraction of electrons transferred (ΔN).

Ionization potential (*I*) and electron affinity (*A*) are related[22]in turn to E_{HOMO} and E_{LUMO} as follows:

$I = -E_{HOMO}$

$A = -E_{LUMO}$

The absolute electronegativity χ and the absolute hardness η are related[23] in turn to IE and EA as follows:

$$\chi = \frac{I + A}{2} \qquad (1)$$

$$\eta = \frac{I - A}{2} \qquad (2)$$

The global electrophilicity index was introduced by Parr[24] and is given by:

$$\omega = \frac{\chi 2}{2\eta} \qquad (3)$$

The number of transferred electrons (ΔN) was also calculated depending on the quantum chemical method[25], [26] by using the equation;

$$\Delta N = \frac{\chi_{Fe} - \chi_{inh}}{2(\eta_{Fe} + \eta_{inh})} \qquad (4)$$

Where χ_{Fe} and χ_{inh} denote the absolute electronegativity of iron and inhibitor molecule η_{Fe} and η_{inh} denote the absolute hardness of iron and the inhibitor molecule respectively. In this study, we use the theoretical value of χ_{Fe} =7.0 eV and $\eta_{Fe} = 0$, for calculating the number of electron transferred.

RESULTS AND DISCUSSION

Polarization results

Fig. 2 shows the potentiodynamic polarization curves for mild steel in 2.0 M H_3PO_4 solutions in the absence and presence of different concentrations of SMP. Electrochemical parameters such as corrosion potential (E_{corr}), corrosion current density (i_{corr}), cathodic Tafel slope (b_c) acquired from extrapolation of polarization curves, as well as the inhibition efficiency ($\eta\%$) of SMP are given in Table 1. The inhibition efficiency was calculated using the following equation:

$$\eta_{PDP}(\%) = \frac{I_{corr} - I_{corr(i)}}{I_{corr}} \times 100 \qquad (5)$$

Where I_{corr} and $I_{corr\ (i)}$ are the corrosion current densities for mild steel electrode in the uninhibited and inhibited solutions, respectively.

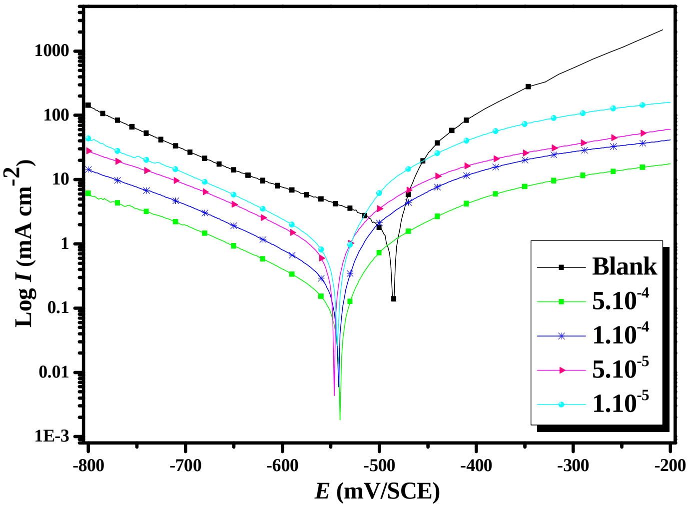

Figure 2. Potentiodynamic polarization curves of carbon steel in 2.0 M H_3PO_4 in the presence of different concentrations of SMP

Table1. Electrochemical parameters of carbon steel at various concentrations of SMP in 2.0 M H_3PO_4 and corresponding inhibition efficiency

Inhibitor	Concentration (M)	E_{corr} vs. SCE (mV)	$-\beta_c$ (mV dec^{-1})	I_{corr} (µA cm^{-2})	η_{Tafel} (%)
Blank	2.0	-488	135	2718	—
SMP	5×10^{-4}	-545	148	174	93.6
	1×10^{-4}	-447	147	364	86.6
	5×10^{-5}	-548	149	832	69.4
	1×10^{-5}	-551	149	1118	58.8

From Fig. 2, obviously, both anodic and cathodic reactions of corrosion process of mild steel electrode were inhibited after adding SMP into the acidic solution. The presence of SMP in the acidic solution results in a slight shift of corrosion potential towards more negative in comparison to that in its absence, and the values of corrosion potential nearly remain constant with the addition of different concentration of SMP. These results indicate that SMP acts as a mixed-type inhibitor with predominant cathodic effectiveness[27]. The parallel cathodic Tafel lines and the almost constant cathodic Tafel slopes in Table 1 suggest that the cathodic process, the hydrogen evolution reaction, is activation-controlled and the addition of SMP does not modify the mechanism of this process[28]. It follows from the date of Table 1 that the corrosion current, i_{corr} decreases, while *IE* (%) enhances with increase in inhibitor concentration. The decrease in the corrosion current density was observed for the SMP, corresponding to a maximum efficiency of 93. 6% at 5×10^{-4} M.

Electrochemical impedance spectroscopy measurements

The corrosion behavior of mild steel in 2.0 M H_3PO_4 without and with various concentrations of SMP at 303 K was investigated using EIS. Nyquist plots are shown in Fig. 3. These diagrams merely present a capacitive loop in the first quadrant, indicating that there is only one time constant. As shown in Fig. 3, the capacitive loops are slightly depressed as semi-circular shapes because of the roughness and other in homogeneities of mild steel surface resulting in a phenomenon called “dispersing effect”[29], [30]. It is apparent that the impedance response of mild steel has significantly changed after the addition of our molecule. The diameters of those loops increase with increasing concentrations of studied compound.

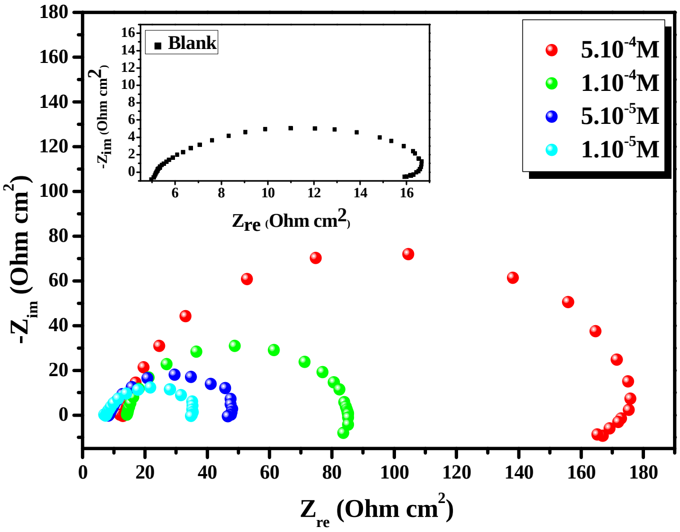

Figure 3. Nyquist diagrams of carbon steel with different concentrations of SMP at 298K

The impedance data are analyzed based on the electrochemical equivalent circuit shown in Fig. 4. R_s represents the electrolyte resistance, R_{ct} is the charge transfer resistance, CPE represents constant phase element to replace a double layer capacitance (C_{dl}) for more accurate fit. The impedance of a constant phase element is described by the expression[31]:

$$Z_{CPE} = \frac{1}{Q(j\omega)^n} \qquad (6)$$

Where Q is the CPE constant (in Ω^{-1} S^n cm^{-2}), ω is the angular frequency (in rad s^{-1}), j2 = -1 is the imaginary number and n is a CPE exponent which can be used as a gauge for the heterogeneity or roughness of the surface. The impedance parameters derived from these plots are given in Table 2. The double layer capacitance (C_{dl}) and inhibition efficiency (η) are defined as follows[32]:

$$C_{dl} = \left(Q.R_{ct}{}^{1-n}\right)^{1/n} \qquad (7)$$

$$\eta_{EIS}(\%) = \left(\frac{R_{ct} - R^{\circ}_{ct}}{R_{ct}}\right) \times 100 \qquad (8)$$

where $R°_{ct}$ and R_{ct} are the charge transfer resistances without and with various concentrations of inhibitors respectively.

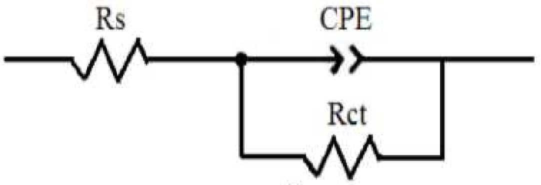

Figure 4. Equivalent electrical circuit corresponding to the corrosion process on the carbon steel in hydrochloric acid

Table2. Electrochemical Impedance parameters for corrosion of carbon steel in acid medium at various contents of SMP

Inhibitor	Concentration (M)	R_t (Ω cm^2)	$Y_0 \times 10^{-5}$ (sn Ω^{-1}cm^{-2})	n	C_{dl} (μF/cm^2)	η_{EIS} (%)
Blank	2.0	14	21.024	0.88	94.96	—
SMP	5×10^{-4}	165.3	2.1629	0.91	12.39	91.5
	1×10^{-4}	71.1	2.6789	0.91	14.42	80.3
	5×10^{-5}	46.7	4.4834	0.90	22.59	70.0
	1×10^{-5}	34.9	6.0218	0.88	25.98	59.9

By increasing the inhibitor concentration the R_{ct} values increase but C_{dl} values decrease. The double layer between the charged metal surface and the solution is considered as an electrical capacitor. The decrease in the C_{dl} value is due to the adsorption of the inhibitors on the steel surface, which displace the water molecule and others ions originally adsorbed on the surface. The adsorption of the inhibitor on mild steel surface can occur either directly on the basis of donor–acceptor interaction between the π electrons (of the double bonds, sulphur, Nitrogen and Oxygen) and the vacant d-orbitals of steel surface atoms[33]–[35]. The inhibition efficiencies calculated from ac impedance results show the same trend as those obtained from polarization curves measurements.

Weight loss tests

The inhibition efficiency ($\eta\%$) and corrosion rate (CR) with different concentrations of SMP for mild steel in 2.0 M H3PO4 solution at 303 K were summarized in Table 3. The inhibition efficiency was calculated from the following equation:

$$\eta_w(\%) = \frac{C_R - C_{R(inh)}}{C_R} \times 100 \qquad (9)$$

Where C_R and $C_{R(inh)}$ represent the corrosion rates in the absence and presence of **SMP**.

Table3. Effect of SMP concentration on corrosion data of carbon steel in 2.0 M H_3PO_4

Inhibitor	Conc. (M)	A (mg cm^{-2} h^{-1})	η_w (%)	(θ)
Blank	2.0	1.972	-	-
SMP	5×10^{-4}	0.1933	90.2	0.902
	1×10^{-4}	0.3293	83.3	0.833
	5×10^{-5}	0.5246	73.4	0.734
	1×10^{-5}	0.7671	61.1	0.611

It is very clear from Table 3 that the corrosion rate of mild steel decreases sharply and the inhibition efficiency increases when the concentration of SMP increases. Maximum inhibition efficiency is attained in the presence of 5.10^{-4} M SMP. These results indicate that SMP is an excellent corrosion inhibitor for mild steel in hydrochloric acid.

Effect of temperature

The effect of temperature on the inhibitive performance of SMP for MS in 2.0 M H_3PO_4 was studied by electrochemical measurements at 5.10^{-4} M concentration of SMP. It is apparent from Table 4that the inhibition efficiency decreases with increase in temperature from 298 to 328 K. The inhibition efficiency decreases with rise in temperature from 93.6% to 79.3%. It can be concluded that the extent of adsorption decreases with rise in temperature whereas the extent of desorption increases.

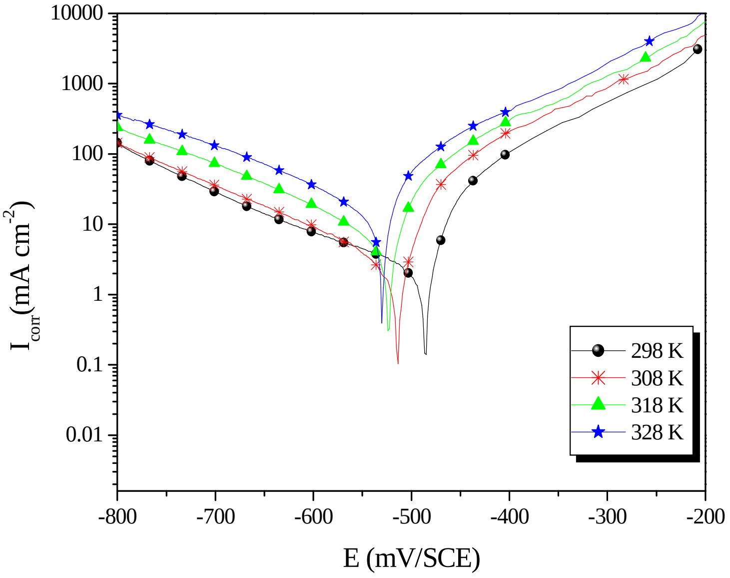

Figure 5. Potentiodynamic polarisation curves of carbon steel in 2M H_3PO_4 at different temperatures

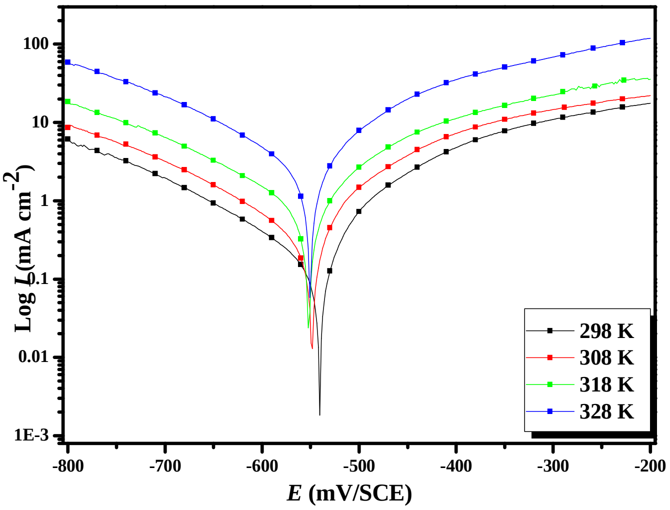

Figure 6. Potentiodynamic polarisation curves of carbon steel in 2M H_3PO_4 in the presence of 5.10^{-4} M of SMP at different temperatures

Table4. Various corrosion parameters for carbon steel in 2M H_3PO_4 in absence and presence of optimum concentration of SMP at different temperatures

Inhibitor	Temperature K	E_{corr} vs. SCE(mV)	$-\beta_c$ (mV dec^{-1})	i_{corr} (μA cm^{-2})	η_{Tafel} (%)
Blank	298	-488	135	2718	-
	308	-532	137	4220	-
	318	-523	132	6610	-
	328	-514	139	11890	-
5×10^{-4}M SMP	298	-545	148	174	93.6
	308	-553	168	406	90.4
	318	-557	161	806	87.8
	328	-555	154	2459	79.3

Some information on the mechanism of the inhibitor action can be obtained by comparing apparent activation energy (Ea), obtained in the presence of inhibitor with that in its absence. The values of Ea were calculated using Arrhenius equation[36]

$$i_{corr} = k \, exp\left(\frac{-E_a}{RT}\right) \qquad (10)$$

Where i_{corr} is the current density rate, R the gas constant, T the absolute temperature, A the pre-exponential factor, The plots of Ln (i_{corr}) versus 1/T without and with inhibitor gave straight lines (Fig. 7). The values of Ea calculatedfrom the slopes of the straight lines are recorded in Table 5. Higher value of activation energy in presence of SMP can be attributed to an appreciable decrease in the adsorption of the inhibitor on the mild steel surface with increase in temperature [37]. It is further noted that the observed value of Ea in presence of the inhibitor at each concentration is greater than that in its absence. The value of standard enthalpy of activation (ΔH_a°) and standard entropy of activation (ΔS_a°) for the dissolution of MS were calculated using the following equation [38]:

$$i_{corr} = \frac{RT}{Nh} \exp\left\{\frac{\Delta S_a^0}{R}\right\} \exp\left\{-\frac{\Delta H_a^0}{RT}\right\} \qquad (11)$$

Where, h is the Planck's constant, N is the Avogadro's number, R is the molar gas constant and T is the absolute temperature.

Straight lines were obtained with a slope and an intercept (Fig. 8) from which the values of ΔHa and ΔSa and were calculated and listed in Table 5. The positive sign of ΔHa reflect the endothermic nature of the steel dissolution process in HCl solution and means that the dissolution of steel is difficult and the decrease in ΔSa in the presence of **SMP** implies a decrease in disordering takes place on going from reactants to the activated complex [39].

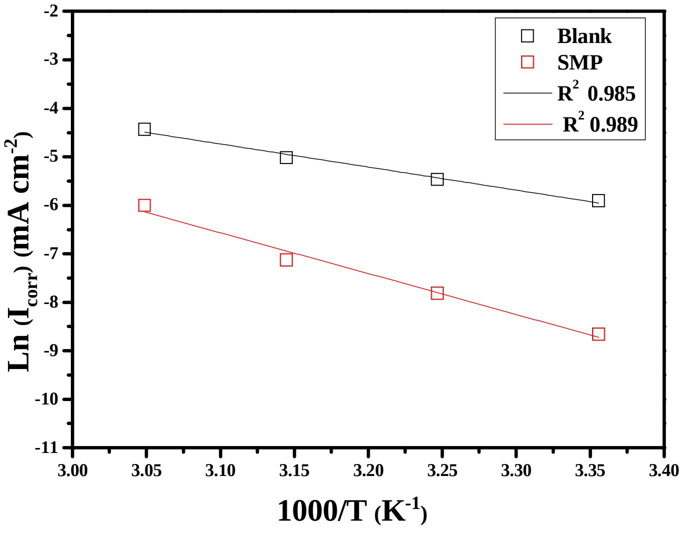

Figure 7. Arrhenius plots of carbon steel in 2.0 M H_3PO_4 with and without 5.10^{-4} M of SMP

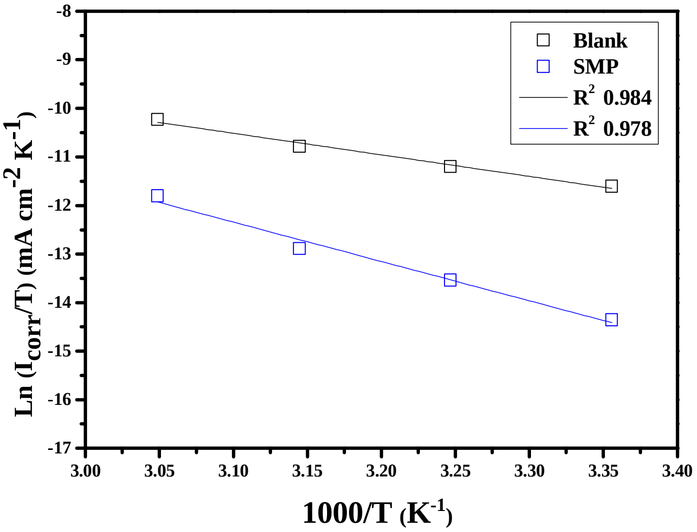

Figure 8. Arrhenius plots of carbon steel in 2.0 M H_3PO_4 with and without 5.10^{-4} M of SMP

Table5. The values of activation parameters E_a, ΔH_a and ΔS_a for carbon steel in 2.0 M H_3PO_4 in the absence and presence of 5.10^{-4} M of SMP

Concentration (M)	E_a (kJ mol^{-1})	ΔH_a (kJ mol^{-1})	ΔS_a (J mol^{-1} K^{-1})	E_a-ΔH_a (kJ mol^{-1})
Blank	39.50	36.91	-112.98	2.59
5×10^{-4}M SMP	69.96	67.36	-91.34	2.60

Adsorption considerations

In order to clarify the nature and the strength of the adsorption of SMP on mild steel, the experimental results were fitted to a series of adsorption isotherms, and Frumkin. The best description of the adsorption behavior of SMP is explained by Langmuir adsorption isotherm, which is given by Eq. (12) [40].

$$\frac{C}{\theta} = \frac{1}{K_{ads}} + C \qquad (12)$$

Where, C is the concentration of the inhibitor, K_{ads} is the equilibrium constant of adsorption and θ is the surface coverage. The Langmuir approach is based on a molecular kinetic model of the adsorption–desorption process. On the other hand, the adsorption equilibrium constant (K_{ads}) is related to the standard free energy of adsorption ($\Delta G°_{ads}$) of the inhibitor molecules by the following Eq. (13)[41]:

$$K_{ads} = \frac{1}{55.5}\exp\left(\frac{-\Delta G^0_{ads}}{RT}\right) \qquad (13)$$

Where R is the universal gas constant, the thermodynamic temperature and the value of 55.5 is the concentration of water in the solution. The results are presented in Table 6.

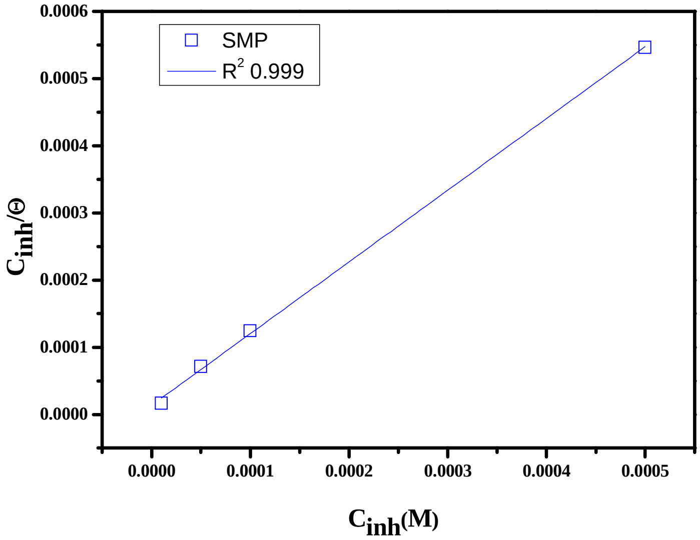

Figure 9. Adsorption isotherm according to Langmuir's model derived from *EIS* measurement

Table 6. Thermodynamic parameters for the adsorption of SMP in 2.0 M H_3PO_4on the carbon steel at 298K.

Inhibitor	Slope	$K_{ads}(M^{-1})$	$\Delta G°_{ads}$(kJ/mol)
SMP	1.06	73837.79	**37.72**

The value of the K_{ads} is 73837.79 M^{-1} which reflects the high adsorption ability of the SMP molecule on the mild steel surface. Generally It is usually accepted that value more negative than −40 kJ/mol involve charge sharing or charge transfer between the metal surface and organic molecules (chemisorption process) while those around −20 kJ/mol or lower is attributed to electrostatic attraction between the charge metal surface and the charged organic molecule in the solution[42, 43]. TheΔG_{ads}° value is negative and high (−37.72 kJ mol^{-1}) indicates the strong interactions between the inhibitor molecules and the metal surface. Therefore, it is concluded that chemical and physical adsorption can be occur for the adsorption of the SMP molecule on the mild steel surface [44, 45].

Quantum chemical calculation

The quantum chemical calculations serve as a theoretical model for establishing a correlation between molecular structure and corrosion inhibition efficiency. Recently, *DFT* has been used to analyze the characteristics of the inhibitor/surface interaction and to describe the structural dependence of the inhibitor on corrosion inhibition process. The *DFT* calculations and correlations were performed on neutral forms of SMP in order to get a better understanding of the influence of the acidic medium in the MS corrosion protection mechanism.

According to the frontier molecular orbital theory (*FMO*) of chemical reactivity, the formation of a transition state is due to an interaction between the frontier orbitals (HOMO and LUMO) of reacting species. Therefore, only the HOMO and LUMO of both reactants are considered when analyzing the chelation processes of adsorption[46, 47]. The difference between the energy levels of these orbitals is important in the evaluation of inhibition potential. The smaller the orbital energy gap (ΔE) between the participating HOMO and LUMO, the stronger are the interactions between two reacting species which cause the adsorption of the inhibitor on the metal surface[48]. The equilibrium geometry structures and the frontier molecule orbital density distributions of the molecule are shown in Fig.10, and the quantum chemical parameters are listed in Table 7.

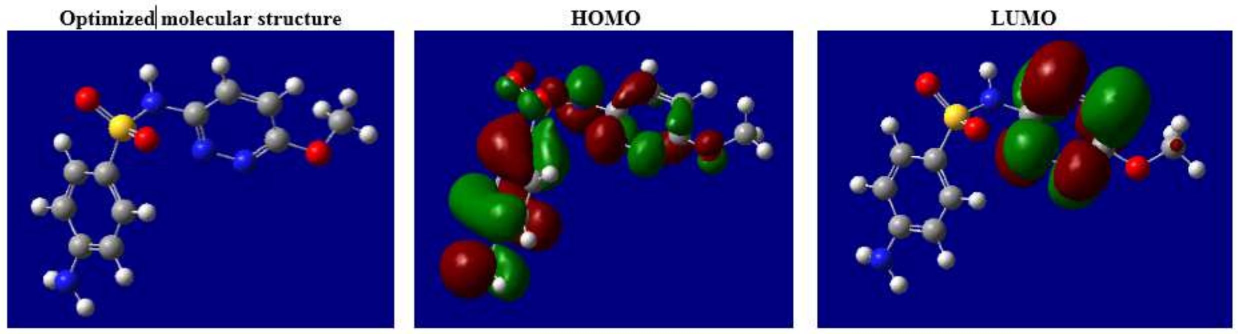

Figure10. Optimized structure and frontier molecular orbital diagrams of SMP by B3LYP/6-31G (d,p)

Table6. Quantum chemical parameters for SMP calculated using B3LYP/6-31G (d,p)

Molecular parameters	**SMP**
E_{HOMO} (eV)	-6.03303949
E_{LUMO} (eV)	-1.69799136
ΔE_{gap} (eV)	4.33504813
μ (debye)	6.7305
I (eV)	6.03303949
A (eV)	1.69799136
χ (eV)	3.86551543
η (eV)	2.16752407
ω	16.1937994
ΔN	0.72305646
TE (a.u)	-1269.4

E_{HOMO} is often associated with the capacity of a molecule to donate electron. High value of E_{HOMO} is likely to indicate a tendency of the molecule to donate electrons to appropriate acceptor molecules with low energy and empty molecular orbital [48]. E_{LUMO} indicates the ability of the molecule to accept electrons. The lower the value of E_{LUMO}, the more probable it is that the molecule would accept electrons [49]. From Table 7, the E_{HOMO} and E_{LUMO} values *suggests* there is a high interactions involved in the corrosion inhibition process. According to frontier orbital theory, the reaction of reactants mainly occurs on HOMO and LUMO. So, the smaller the gap (ΔE) between E_{HOMO} and E_{LUMO} is, the more probable it is to donate and accept electrons. The value of ΔE in Table 7, suggest the strongest ability of SMP to form coordinate bonds with *d*-orbitals of metal through donating and accepting electrons, is in good agreement with the experimental results [50]. Additionally, for the dipole moment, higher values of μ will favor the enhancement of corrosion inhibition [51]. From Table 7, the values of μ support the experimental results mentioned above.

Another method to correlate inhibition efficiency with parameters of molecular structure is to calculate the fraction of electrons transferred from inhibitor to metal surface. The calculated result are presented in Table 7. Generally, value of ΔN shows inhibition efficiency resulted from electron donation, and the inhibition efficiency increases with the increase in electron-donating ability to the metal surface in the case of ΔN less than 3.6. In this study, it can be seen from Table 7 that the value of ΔN indicate the high ability of SMP to donate electrons to the metal surface, which is in good agreement with the order of inhibition efficiency of this inhibitor [52, 53].

CONCLUSION

The studied compound, Sulfamethoxypyridazine, exhibit good inhibition properties for the mild steel corrosion in 2 M H_3PO_4, the inhibition efficiency increases on increasing concentration of the inhibitor and decreases with increase in temperature. The potentiodynamic polarization curves show that the Sulfamethoxypyridazine prevent metal dissolution and also hydrogen evolution reactions (mixed-type inhibitor).The adsorption of SMP was successfully described by the Langmuir adsorption isotherm and the corresponding value of $\Delta G_{ads}°$ reveal that the adsorption mechanism of this inhibitor on mild steel surface in 2 M H_3PO_4 solution is a mixed type involving both physisorption and chemisorption. Through DFT quantum-chemical calculations a correlation between, parameters related to the electronic structure of studied inhibitor and their potential to inhibit the corrosion process, could be established.

Acknowledgment

The authors would like to thank the Palestenian Ministry of Higher Education for their support.The support given through an“INCRECYT” research contract to M. Zougagh is also acknowledged.

REFERENCES

[1] Solmaz R, Kardaş G, Yazici B, Erbil M, *Colloids Surf. A*,**2008**, 7, 312.
[2] Prajila M, Sam J, Bincy J, Abraham J, J. *Mater. Environ. Sci*,**2012**, 3,1045.
[3] Naik U J,Panchal V A, Patel A S, Shah N K, *J. Mater. Environ. Sci*,**2012**, 3, 935.
[4] M Larouj, MBelayachi, H Zarrok, A Zarrouk, A Guenbour, M Ebn Touhami, A Shaim, S Boukhriss, H Oudda, B Hammouti, *Der PharmaChemica*, **2014**, 6, 3,373-384.
[5] M Larouj, H Lgaz, H Zarrok, H Serrar, H Zarrok, H Bourazmi, A Zarrouk, A Elmidaoui, A Guenbour, S Boukhris and H Oudda, *Journal of Material and Environmental Science*,**2015**, 6, 11, 3251-3267.
[6] M Larouj, M Belkhaouda, H Lgaz, R Salghi, S Jodeh, S Samhan, H Serrar, S Boukhris, M Zougagh and H Oudda, *Der PharmaChemica*, **2016**, 8, 2, 114-133.
[7] H Lgaz, O Benali, R Salghi, S Jodeh, M Larouj, O Hamed, M Messali, S Samhan, M Zougagh and H Oudda, *Der PharmaChemica*, **2016**, 8, 2, 172-190.
[8] Ben Hmamou D, Salghi R, Zarrouk A, Zarrok H, Hammouti B, Al-Deyab S S, Bouachrine M, Chakir A, Zougagh M, *Int. J. Electrochem. Sci*,**2012**, 7, 5716.
[9] L Afia, M Larouj, H Lgaz, R Salghi, S Jodeh, S Samhan and M Zougagh, *Der PharmaChemica*, **2016**, 8, 2, 22-35.
[10] B El Makrini, M Larouj, H Lgaz, R Salghi, A Salman, M Belkhaouda, S Jodeh, M Zougagh and H Oudda, *Der PharmaChemica*, **2016**, 8, 2, 227-237.
[11] B El Makrini, H Lgaz, M Larouj, R Salghi, A Rasem Hasan, M Belkhaouda, S Jodeh, M Zougagh and H Oudda, *Der PharmaChemica*, **2016**, 8, 2, 256-268.
[12] Ben Hmamou D, Salghi R, Zarrouk A, Zarrok H, Al-Deyab S S, Benali O, Hammouti B, *Int. J. Electrochem*. Sci,**2012**, 7, 8988.
[13] H Lgaz, Y ELaoufir, Y Ramli, M Larouj, H Zarrok, R Salghi, A Zarrouk, A Elmidaoui, A Guenbour, EL M Essassi and H Oudda, *Der PharmaChemica*, **2015**, 7, 6, 36-45.
[14] Ben Hmamou D, Aouad M R, Salghi R, Zarrouk A, Assouag M, Benali O, Messali M, Zarrok H, Hammouti B, *J. Chem. Pharm. Res*,**2012**, 4, 3489.
[15] M Belayachi, H Zarrok, M Larouj, A Zarrouk, H Bourazmi, A Guenbour, B Hammouti, SBoukhriss, H Oudda, *Phys. Chem. News*,**2014**, 74, 85-93.
[16] F Bentiss, M Lagrenee, MTraisnel, *Corrosion*, **2000**, 56, 733.
[17] F Bentiss, M Traisnel, M Lagrenee, *J. Appl. Electrochem*,**2001**, 31, 41.
[18] A D Becke, *J. Chem. Phy*, **1992**, 96, 9489.
[19] A DBecke, *J. Chem. Phy*, **1993**, 98, 1372.
[20] C Lee, W Yang, R G Parr, *Phy. Rev. B*, **1988**, 37, 785.
[21] M J Frisch et al Gaussian 03, Revision C.02, Gaussian Inc., Pittsburgh, PA, **2003**.
[22] M J S Dewar, W Thiel, *J. Am. Chem. Soc*, **1977**, 99, 4899.
[23] R G Pearson, *Inorg. Chem*, **1988**, 27, 734.
[24] V S Sastri, J R Perumareddi, *Corrosion*, **1997**, 53, 671
[25] V S Sastri, J RPerumareddi, *Corrosion* (NACE) **1997**, 53, 617.
[26] I Lukovits, E Kalman, F Zucchi, *Corrosion* (NACE) **2001**, 57, 3.
[27] A Bousskri, A Anejjar, M Messali, R Salghi, O Benali, Y Karzazi, S Jodeh, M Zougagh, E EEbenso, et BHammouti, *J. Mol. Liq*, **2015**, 211, 1000‑1008.
[28] N S Patel, J Hadlicka, P Beranek, R Salghi, H Bouya, H A Ismat, et BHammouti, *Port. Electrochimica Acta*, **2014**, 32, 6, 395‑403.
[29] L Bammou, M Belkhaouda, R Salghi, O Benali, A Zarrouk, H Zarrok, et BHammouti, *J. Assoc. Arab Univ. Basic Appl. Sci*, **2014**, 16, 83‑90.
[30] R Salghi, L Bazzi, B Hammouti, S Kertit, A Bouchtart, et Z El Alami, présenté à Annales de Chimie Science des Materiaux, **2000**, 25, 593‑600.
[31] R Salghi, L Bazzi, B Hammouti, S Kertit, A Bouchtart, et Z El Alami, *Ann. Chim. Sci. Matér*, **2000**, 25, 8, 593‑600.
[32] R Salghi, L Bazzi, et MZaafrani, *Acta Chim. Slov*, **2003**, 50, 3, 491‑504.
[33] D B Hmamou, R Salghi, A Zarrouk, M R Aouad, O Benali, H Zarrok, M Messali, B Hammouti, M MKabanda, et MBouachrine, *Ind. Eng. Chem. Res*, **2013**, 52, 40, 14315‑14327.
[34] R N Singh, A Kumar, R K Tiwari, et PRawat, *Spectrochim. Acta. A. Mol. Biomol. Spectrosc.***2013**, 112, 182‑190.
[35] H Jafari, I Danaee, H Eskandari, et MRashvandAvei, *J. Mater. Sci. Technol*, **2014**, 30, 3, 239‑252.
[36] C Verma, M A Quraishi, et A Singh, *J. Mol. Liq.*, **2015**, 212, 804‑812.
[37] C Verma, E EEbenso, I Bahadur, I B Obot, et M AQuraishi, *J. Mol. Liq*, **2015**, 212, 209‑218.
[38] C Verma, M A Quraishi, et A Singh, *J. Taiwan Inst. Chem. Eng*, **2016**, 58, 127‑140.

[39] D Daoud, T Douadi, H Hamani, S Chafaa, et M Al-Noaimi, *Corros. Sci*, **2015**, 94, 21‑37.

[40] M V Fiori-Bimbi, P E Alvarez, H Vaca, et C AGervasi, *Corros. Sci*, **2015**, 92, 192‑199.

[41] I Lukovits, E Kalman, et F Zucchi, *Corrosion*, **2001**, 57, n^{o} 1, p. 3‑8.

[42] S Kharchouf, L Majidi, M Bouklah, B Hammouti, A Bouyanzer, et AAouniti, *Arab. J. Chem*, **2014**, 7, 5, 680‑686.

[43] K Ramya, R Mohan, K KAnupama, et A Joseph, *Mater. Chem. Phys*, **2015**, 149‑150, 632‑647.

[44] I B Obotet AMadhankumar, *J. Ind. Eng. Chem*, **2015**, 25, 105‑111.

[45] R Yıldız, T Doğan, et İDehri, *Corros. Sci*, **2014,** 85, 215‑221.

[46] L Feng, H Yang, et F Wang, *Electrochimica Acta*, **2011**, 58, 427‑436.

[47] A Biswas, S Pal, et GUdayabhanu, *Appl. Surf. Sci*, **2015**, 353, 173‑183.

[48] Bouklah M, Benchat N, Aouniti A, Hammouti B, Benkaddour M, Lagrenée M, Vezin H, Bentiss F, Prog. Org. Coat,**2004**, 51,118-124

[49] K F Khaled, *ElectrochimicaActa*, **2010**, 55, 22, 6523‑6532.

[50] N A Odewunmi, S A Umoren, et Z MGasem, *J. Environ. Chem. Eng*, **2015**, 3, 1, 286‑296.

[51] N O Eddy, H Momoh-Yahaya, et E EOguzie, *J. Adv. Res*, **2015**, 6, 2, 203‑217.

[52] D Zhang, Y Tang, S Qi, D Dong, H Cang, et G Lu, *Corros. Sci*, **2016**, 102, 517‑522.

[53] M H Hussin, A A Rahim, M N Mohamad Ibrahim, et N Brosse, *Measurement*, **2016**, 78, p. 90‑103.